JOURNAL OF COMPUTATIONAL PHYSICS **16**, 32–48 (1974)

A Discretized Solution for the Solitary Wave

ROBERT K.-C. CHAN

Science Applications, Inc., La Jolla, California

Received March 4, 1974

A successive correction technique, based on generalization to n dimensions of Newton's process for finding zeros of a real function of a real variable, is employed to solve two-dimensional steady-state potential flows with free surface and gravity. The fluid domain in the physical plane is mapped into the complex potential (φ, ψ) plane where the solution for the vertical coordinate $y(\varphi, \psi)$ is sought. A specific application to the analysis of large-amplitude solitary waves has been made; the results are in good agreement with experiments.

1. INTRODUCTION

The phenomenon of a solitary wave traveling in a rectangular channel of uniform depth was first reported by John Scott Russell in 1834. Russell defined the solitary wave as a single elevation above the surrounding undisturbed water level, neither followed nor preceded by any other elevation or depression of the surface, producing a definite transport in the direction of wave propagation only, and traveling without change of shape and with essentially constant velocity throughout the observable time of travel [1]. Subsequent analytic studies were made by Saint Venent, J. Boussinesq, Lord Rayleigh, G. G. Stokes, J. McCowan [1] and others. Recent investigations include Laitone's [2] higher-order theory, Grimshaw's [3] third-order theory, and Fenton's [4] ninth-order solution.

The most convenient coordinate system to describe the solitary wave in an infinitely long channel of constant depth is one that moves at the same speed as the wave. Because of the constant speed and shape of the wave, this choice of coordinate system reduces the time-dependent problem to a steady-state problem. The effect of viscosity is believed to be negligible. Thus, the flow is assumed to be invicid, irrotational, and incompressible; this permits a formulation in terms of the velocity potential φ (Fig. 1).

For two-dimensional potential flows we have the following relationships:

$$u = \partial\varphi/\partial x = \partial\psi/\partial y \tag{1}$$

and

$$v = \partial\varphi/\partial y = -\partial\psi/\partial x, \tag{2}$$

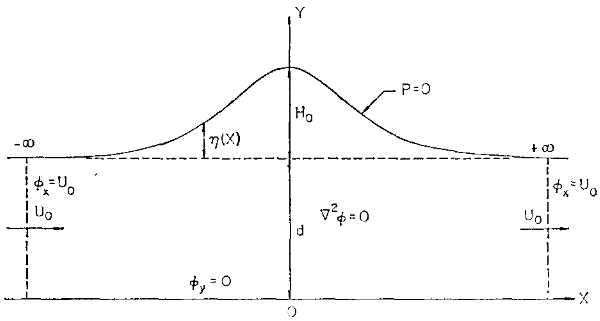

FIG. 1. Definition sketch.

where u is the velocity component in the x-direction, v is the velocity component in the y-direction, and ψ is the stream function. Within the fluid, the governing equation is the Laplace equation

$$(\partial^2\varphi/\partial x^2) + (\partial^2\varphi/\partial y^2) = 0. \tag{3}$$

On the channel floor, the condition that velocity component normal to a rigid boundary must vanish is expressed by

$$\partial\varphi/\partial y = 0, \qquad \text{at} \qquad y = 0. \tag{4}$$

At infinity the flow is essentially uniform; thus,

$$\partial\varphi/\partial x = U_0, \qquad x = \pm\infty \tag{5}$$

where U_0 is the speed of the uniform flow and is the same as the speed of the wave when observed from a fixed coordinate system.

The free-surface condition is simply that the pressure must be a constant, or $p = 0$ if zero is chosen as the constant. To express this condition in terms of the velocity potential, the Bernoulli equation is used:

$$(1/2)[(\partial\varphi/\partial x)^2 + (\partial\varphi/\partial y)^2] + gy = B_0 = (U_0^2/2) + gd \tag{6}$$

at $y = \eta + d$, where η is the free-surface elevation measured upward from the water level at infinity (where the water depth is d), g is the acceleration due to gravity, and B_0 is the Bernoulli constant. Equation (6) is a nonlinear boundary condition which accounts for the major difficulty of the problem. Because of this nonlinearity, analytic theories so far available are approximate to varying degrees. Their validity is necessarily limited by the approximations made.

Daily and Stephan [1] conducted a series of careful experiments to determine the profile and speed of the solitary wave and some information about the interior fluid motion in the wave. Their experimental data indicate that the analytic theories are generally adequate for waves of moderate or small amplitudes. For larger amplitudes, theoretical results diverge from those of the experiments. For example, Daily and Stephan showed the profile given by Boussinesq's theory is the most satisfactory among the analytic results for the height-to-depth ratio H_0/d less than about 0.4. A significant discrepancy between Boussinesq's profile and the experiments was found for larger values of H_0/d (Fig. 2).

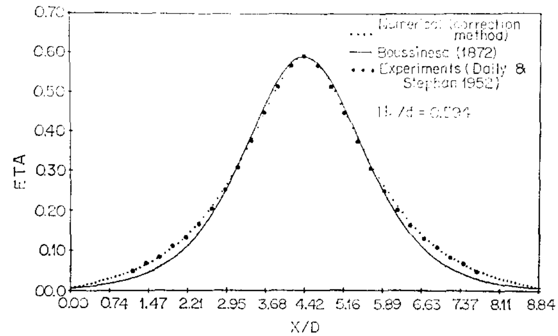

FIG. 2. Comparison of wave profiles.

In view of the inherent difficulties in handling nonlinear problems by analytic approaches, a number of numerical studies have been undertaken in the past few years. Of particular value in treating two-dimensional, steady, free-surface flows under the influence of gravity is the use of the x and y coordinates as dependent variables and the velocity potential φ and the stream function ψ as independent variables. The flow region then becomes a rectangle in the complex potential plane (Figs. 3 and 4) and the boundary geometry is greatly simplified. However, the

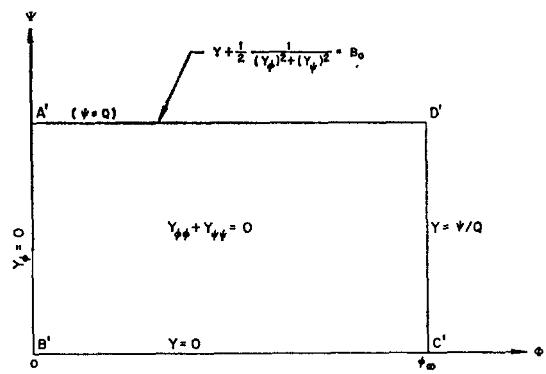

FIG. 3. The complex potential plane.

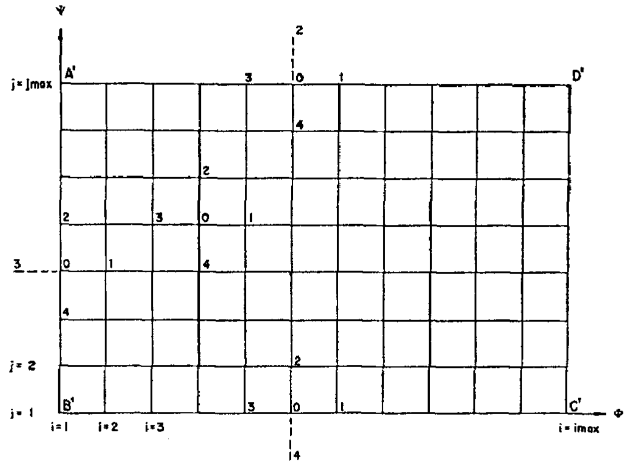

FIG. 4. The finite-difference mesh.

nonlinearity of the problem remains to be the major difficulty in obtaining solutions. By formulating the problem in the $\varphi - \psi$ plane, Strelkoff [5] obtained solutions to the solitary wave by solving an integro-differential equation. Byatt-Smith [6] independently took a similar approach in obtaining profiles for the solitary wave of less than maximum height.

In this paper, the solitary wave problem is solved by using a successive correction method which may have wide application in the study of two-dimensional, steady potential flows with free surfaces. The numerical procedure involved is presented in a form suitable for calculation on a digital computer.

2. Formulation of the Problem

The concepts to be developed here are best illustrated by an example for the reason that some of the governing equations must be derived specifically to meet the situation of a particular problem. The problem of a steady-state solitary wave was selected for demonstration purposes and the subsequent discussions are presented in the context of this application. However, there is no loss of generality because all of the essential features of the method are developed and utilized.

In this paper, all lengths are nondimensionalized by d, all accelerations by g and consequently, all velocities by $(gd)^{1/2}$. In this dimensionless system, both g and d are unity, and these values are assumed in the following discussions.

2.1. *Formulation in the Physical Plane*

In accordance with the description in Section 1, the two-dimensional flow in a solitary wave relative to a coordinate system fixed in the wave can be described in terms of φ and ψ. Because of the symmetry of the solitary wave, the problem can be analyzed by taking only half of the flow region. The governing equation and pertinent boundary conditions are shown in Fig. 1.

The problem appears well posed and could be considered solved if a function $\varphi(x, y)$ were found to satisfy all the above conditions. Because of the nonlinear characteristic of Eq. (6), an analytic approach is rather difficult. In fact, even a numerical method is difficult to apply in the configuration shown in Fig. 1, because the position of the free surface is not known. Fortunately, we can simplify the problem to a certain extent by using the transformation technique described in the next section.

2.2. *Formulation in the Complex Potential Plane*

By choosing the velocity potential φ and the stream function ψ as the independent variables and regarding the coordinates x and y as the dependent variables, we can transform the problem formulated in the previous section into a less complicated one in the complex potential or the φ–ψ plane (Fig. 3). We use the Implicit Function Theorem [7] to derive the partial derivatives of $x(\varphi, \psi)$ and $y(\varphi, \psi)$.

The Jacobian of the transformation is defined as

$$J = \begin{vmatrix} \partial\varphi/\partial x & \partial\varphi/\partial y \\ \partial\psi/\partial x & \partial\psi/\partial y \end{vmatrix} = q^2 \tag{7}$$

where

$$q^2 = u^2 + v^2. \tag{8}$$

Then, the inverse partial derivatives become

$$\partial x/\partial\varphi = (1/J)(\partial\varphi/\partial x) = (1/J)(\partial\psi/\partial y), \tag{9}$$

$$\partial x/\partial\psi = -(1/J)(\partial\varphi/\partial y) = (1/J)(\partial\psi/\partial x), \tag{10}$$

$$\partial y/\partial\varphi = (1/J)(\partial\varphi/\partial y) = -(1/J)(\partial\psi/\partial x), \tag{11}$$

and

$$\partial y/\partial\psi = (1/J)(\partial\varphi/\partial x) = (1/J)(\partial\psi/\partial y). \tag{12}$$

These inverse partial derivatives will be regular functions in the complex potential plane wherever the Jacobian is not zero. Singularities occur wherever $J = 0$ (i.e., at stagnation points in the flow field). There usually are no stagnation points in a solitary-wave flow. However, when the solitary wave reaches its maximum possible height the horizontal speed of the fluid at the crest in the unsteady flow is equal to the celerity of the wave; in a steady-state configuration, this means that the wave crest is a stagnation point. Thus, Eqs. (9)–(12) hold everywhere in the flow except at the crest of a limit-height wave.

The relations (9)–(12) can be manipulated to yield a formulation of our problem in terms of $y(\varphi, \psi)$ in the complex potential plane. Because the free surface in a steady flow is a streamline along which $\psi =$ constant, the position of the free surface is known in the complex potential plane (Fig. 3) provided that the total flow rate Q per unit breadth of channel is prescribed. The additional advantage is that the flow region becomes rectangular, which is most desirable when finite-difference approximations are employed. In Fig. 3, we have selected the equipotential line which goes through the wave crest as the line $\varphi = 0$. Also, we let $\psi = 0$ along the streamline that coincides with the channel floor and $\psi = Q$ along the free surface.

The boundary conditions can be immediately obtained from their corresponding conditions in the physical plane. The results are shown in Fig. 3. Theoretically, the boundary condition of $C'D'$ must be applied at infinity. The numerical computation, however, has to be carried out in a finite region. Therefore we assume that the condition $\partial\varphi/\partial x = U_0$, which through Eqs. (9)–(12) implies $y = \psi/Q$, can be applied to a finite location $C'D'$ without significant loss of accuracy in the solution if $C'D'$ is far enough from $A'B'$. In actual computation, we first select a location for $C'D'$ and then move $C'D'$ farther in the positive φ-direction until the sequence of solutions converge.

In nondimensional form, the free surface condition Eq. (6) becomes

$$y + (1/2)[(\partial y/\partial\varphi)^2 + (\partial y/\partial\psi)^2]^{-1} = B_0 . \tag{13}$$

Equations (9)–(12) imply that $x(\varphi, \psi)$ and $y(\varphi, \psi)$ are harmonic functions, i.e.,

$$(\partial^2 x/\partial\varphi^2) + (\partial^2 x/\partial\psi^2) = 0 \tag{14}$$

and

$$(\partial^2 y/\partial\varphi^2) + (\partial^2 y/\partial\psi^2) = 0. \tag{15}$$

Because of the presence of y in the free-surface boundary condition, the problem is naturally formulated in terms of the dependent variable $y(\varphi, \psi)$ rather than $x(\varphi, \psi)$.

The complete formulation in the complex potential plane is summarized in Fig. 3. We prescribe the value of Q, which is equal to the wave celerity in nondimensional form, and seek a solution $y(\varphi, \psi)$ in the rectangular domain $A'B'C'D'$. It is seen that the geometry of the fluid domain has been greatly simplified. However, the nonlinearity of the free-surface boundary condition remains. A method of solution employing successive approximations is presented in the following section.

3. Discretized Solution Technique

3.1. *Finite-Difference Representations*

To set up a finite-difference scheme the region $A'B'C'D'$ is subdivided by a rectangular grid (Fig. 4). The horizontal position of the grid points is designated by the index i which runs from 1 to i max, while j, running from 1 to j max, refers to the vertical position of the grid points. These grid points have a horizontal spacing of $\delta\varphi$ and a vertical spacing of $\delta\psi$.

Now Eq. (15) can be written in the finite-difference form

$$((y_1 - 2y_0 + y_3)/(\delta\varphi)^2) + ((y_2 - 2y_0 + y_4)/(\delta\psi)^2) = 0 \tag{16}$$

or

$$2(Z + 1)\, y_0 - y_1 - Zy_2 - y_3 - Zy_4 = 0 \tag{17}$$

for any interior point 0 (Fig. 4), where $Z \equiv (\delta\varphi/\delta\psi)^2$. If the point 0 lies on the boundary $A'B'$, then the boundary condition becomes $y_3 = y_1$ which can be substituted into Eq. (17) to yield

$$2(Z + 1)\, y_0 - 2y_1 - Zy_2 - Zy_4 = 0. \tag{18}$$

At the free surface, Eq. (13) has the finite-difference representation

$$y_0 + \frac{1/2}{((y_1 - y_3)/2\delta\varphi)^2 + ((y_2 - y_4)/2\delta\psi)^2} = B_0\,. \tag{19}$$

However, the y_2 in Eq. (19) lies outside the fluid region (Fig. 4). We may apply Eq. (17) to the point 0 which is at the free surface to obtain an expression for the image value y_2 in terms of y_0, y_1, y_3 and y_4 and Eq. (19) becomes

$$y_0 + (H_V)_0 = B_0 \tag{20}$$

where the "velocity head" $(H_v)_0$ is defined as

$$(H_V)_0 = \frac{1}{2}\left\{\left(\frac{y_1 - y_3}{2\delta\varphi}\right)^2 + \left[\frac{\frac{2(Z+1)}{Z}y_0 - \frac{1}{Z}y_1 - \frac{1}{Z}y_3 - 2y_4}{2\delta\psi}\right]^2\right\}^{-1}. \tag{21}$$

No special treatment is needed for the boundaries $B'C'$ and $C'D'$ where the values of y are fixed throughout the computation.

3.2. *The Correction Equations*

The problem formulated in the last section is nonlinear and no simple methods to obtain a solution are yet known. The method to be discussed here is based on successive correction which is the generalization to n dimensions of Newton's process for finding zeros of a real function of a real variable [8]. First, we guess an approximate solution $y(\varphi, \psi)$. As expected, the governing equation and the boundary conditions are not quite satisfied by this approximation. But we can construct a correction scheme to improve the guessed $y(\varphi, \psi)$ so that the various conditions will be closer to being satisfied.

Let us examine the free-surface condition Eq. (20), which we rewrite in the form

$$y_0 + (H_V)_0 + (H_p)_0 = B_0 \tag{22}$$

where $(H_p)_0$ is the pressure head which should be zero at the free surface. However, $(H_p)_0$ does not, in general, vanish for the guessed $y(\varphi, \psi)$. To make $(H_p)_0 = 0$ everywhere on the free surface we must properly adjust the value of y at every grid point by a small amount. To evaluate how small changes in the guessed y field affect the pressure head $(H_p)_0$, we take the differential of each term in Eq. (22) to obtain

$$\begin{aligned} d(H_p)_0 = &- c_0 + 4(H_V)_0^2 \left\{ \frac{y_\varphi}{2\delta\varphi} (c_1 - c_3) \right. \\ &\left. + \frac{y_\psi}{2\delta\psi} \left[\frac{2(Z+1)}{Z} c_0 - \frac{1}{Z} c_1 - \frac{1}{Z} c_3 - 2c_4 \right] \right\} \end{aligned} \tag{23}$$

where c denotes a small change in y, and

$$y_\varphi = (y_1 - y_3)/2\delta\varphi \tag{24}$$

and

$$y_\psi = \frac{\frac{2(Z+1)}{Z} y_0 - \frac{1}{Z} y_1 - \frac{1}{Z} y_3 - 2y_4}{2\delta\psi} \tag{25}$$

are evaluated using the approximate $y(\varphi, \psi)$. Equation (23) reveals the various contributions to the small change of $(H_p)_0$. Now we let $d(H_p)_0 = -(H_p)_0$ because we wish to reduce $(H_p)_0$ to zero. Then, after rearranging, we have the correction equation for the free surface

$$m_0 c_0 + m_1 c_1 + m_3 c_3 + m_4 c_4 = -(H_p)_0 \tag{26}$$

where

$$m_0 = (2(Z+1)/Z)(2(H_V)_0^2\, y_\psi/\delta\psi) - 1, \tag{26a}$$

$$m_1 = (2(H_V)_0^2\, y_\varphi/\delta\varphi) - (1/Z)(2(H_V)_0^2\, y_\psi/\delta\psi), \tag{26b}$$

$$m_3 = -(2(H_V)_0^2\, y_\varphi/\delta\varphi) - (1/Z)(2(H_V)_0^2\, y_\psi/\delta\psi), \tag{26c}$$

$$m_4 = -(4(H_V)_0^2\, y_\psi/\delta\psi), \tag{26d}$$

and $(H_p)_0$ is evaluated by Eq. (22) using the approximate $y(\varphi, \psi)$.

Next, consider Eq. (17) which governs the interior flow region. We define the residual

$$R_0 \equiv 2(Z+1)\,y_0 - y_1 - Zy_2 - y_3 - Zy_4 \tag{27}$$

where R_0 does not, in general, vanish for the guessed $y(\varphi, \psi)$ field. Using the same idea that led to Eq. (26), we evaluate the differential of each term in Eq. (27) and require that the small changes in y_0, y_1, etc., should be of such magnitude that their combined effect produces $dR_0 = -R_0$. The result is a correction equation for the interior flow region

$$2(Z+1)\,c_0 - c_1 - Zc_2 - c_3 - Zc_4 = -R_0\,. \tag{28}$$

Similarly, referring to Eq. (18), the residual for grid points 0 lying on the boundary $A'B'$ is defined as

$$R_0 \equiv 2(Z+1)\,y_0 - 2y_1 - Zy_2 - Zy_4 \tag{29}$$

and the appropriate correction equation is

$$2(Z+1)\,c_0 - 2c_1 - Zc_2 - Zc_4 = -R_0\,. \tag{30}$$

On the boundaries $B'C'$ and $C'D'$ the values of y need no correction because they are prescribed. Consequently, $c_0 = 0$ is applied there.

The problem of finding $c(\varphi, \psi)$ is linear as all the correction equations are linear. Indeed, we have locally linearized the nonlinear boundary condition on the free surface. For Eq. (26) to be a good approximation, the coefficients given by Eqs. (26a–d) must also be good approximations. In other words, the success of the correction method presented here requires a reasonably good initial guess of $y(\varphi, \psi)$.

Also, it is important to note that we can only deal with *small* corrections. However, this requirement does not limit the applicability of the method. We can always start with a case which contains a small degree of nonlinearity and for which an analytic solution is available. Then, by changing some key parameter (or parameters) the nonlinearity can be increased step by step while at the same time the successive correction method can be applied to obtain the solution for each new step.

3.3. *Solution Techniques*

As soon as the guessed values of $y(\varphi, \psi)$ are stored in the computer, the coefficients of the correction equations, the nonvanishing pressure head $(H_p)_0$ on the free surface and the residual R_0 for interior points and points lying on $A'B'$ can be evaluated. All these quantities are temporarily regarded as constants during the process of finding a solution to the current correction field $c(\varphi, \psi)$.

After $c(\varphi, \psi)$ is found, the initially guessed $y(\varphi, \psi)$ is improved by adding the value of c at each grid point to its corresponding old value of y. The new $y(\varphi, \psi)$ field thus obtained leads to a smaller absolute value of $(H_p)_0$ on the free surface and of R_0 elsewhere, provided that the starting $y(\varphi, \psi)$ was reasonably good and that the $c(\varphi, \psi)$ field was solved quite accurately.

Now, a second correction can be made. First, however, the residuals and coefficients in the correction equation have to be recomputed from the current $y(\varphi, \psi)$ field. They are constants only within the current process of finding $c(\varphi, \psi)$. The computation is terminated when the largest magnitudes of $(H_p)_0$ and R_0 become less than a prescribed small number. The most recently obtained $y(\varphi, \psi)$ field is then taken as the solution.

The method of solving $c(\varphi, \psi)$ deserves some consideration. It is clear that all the correction equations are linear so this is really a problem of solving a set of simultaneous linear algebraic equations. Because the free surface boundary condition for c is of the mixed type, this system of linear equations is quite sensitive and cannot be properly handled by the relaxation method. Consequently, the direct Gauss Elimination Method [8] is employed to solve for $c(\varphi, \psi)$.

Calculating $x(\varphi, \psi)$, $u(\varphi, \psi)$, $v(\varphi, \psi)$ and $p(\varphi, \psi)$ is a relatively simple matter after $y(\varphi, \psi)$ is obtained. Using the Cauchy–Riemann condition $\partial x/\partial\varphi = \partial y/\partial\psi$, which can be derived from Eqs. (9)–(12), we integrate to obtain

$$x = \int_0^\varphi \left(\frac{\partial y}{\partial \psi}\right)_{\psi=\text{constant}} d\varphi, \tag{31}$$

since we have chosen $\varphi = 0$ at $x = 0$. Each horizontal line in the finite-difference mesh (Fig. 4) represents a streamline along which ψ = constant. Evaluation of $\partial y/\partial\psi$ at any grid point can be easily performed with finite differences. The integral in Eq. (31) can be evaluated numerically by using any of the well-established procedures. We selected the Adams–Moulton corrector [9].

By using the computed values of $x(\varphi, \psi)$ and $y(\varphi, \psi)$ to trace the curve along a ψ = constant line, we immediately obtain a streamline in the physical plane. An equipotential line in the physical plane can be similarly obtained by plotting pairs of x and y values related to a vertical line (φ = constant) in the complex potential plane. Figure 5 is an example of such a plot.

The velocity components u and v are calculated by using the inverse partial derivative relations:

$$u = (\partial y/\partial\psi)[(\partial y/\partial\varphi)^2 + (\partial y/\partial\psi)^2]^{-1} \tag{32}$$

and

$$v = (\partial y/\partial\varphi)[(\partial y/\partial\varphi)^2 + (\partial y/\partial\psi)^2]^{-1}. \tag{33}$$

Finally, the pressure distribution in the interior of the flow is obtained from the Bernoulli equation.

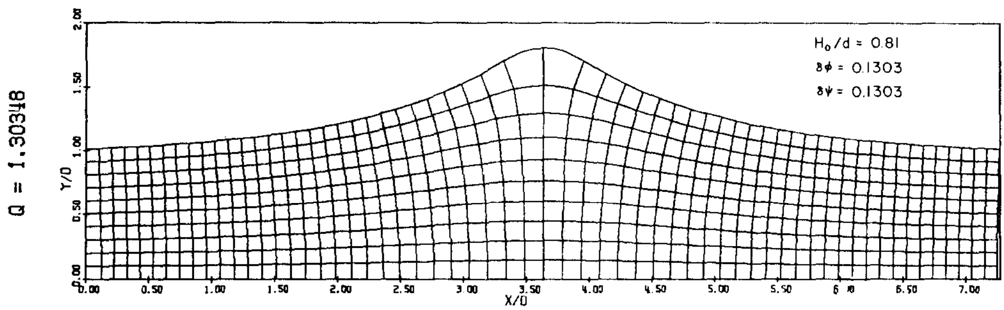

FIG. 5. An example of the computed flow pattern.

4. RESULTS AND CONCLUSIONS

To obtain the solitary wave solutions, it is necessary to devise a systematic way of obtaining a guessed $y(\varphi, \psi)$. Because the nondimensional wave speed or the discharge Q of the steady flow is prescribed, we can compute an approximate value for the wave height H_0 by the well-known formula

$$Q = (1 + H_0)^{1/2} \tag{34}$$

for the speed of a long, finite-amplitude wave [10]. Next, we want to find an approximate distribution of y along the free surface $A'D'$ (Fig. 3). There,

$$v/u = dy/dx. \tag{35}$$

But $\varphi = \varphi(x, y)$. Taking the differential of φ, we get

$$d\varphi = u\,dx + v\,dy. \tag{36}$$

Eliminating v between Eqs. (35) and (36) leads to

$$dx/d\varphi = 1/u[1 + (dy/dx)^2], \tag{37}$$

where u can be estimated as the average horizontal velocity Q/y, which is a reasonable approximation for $H_0 < 0.3$. Thus, Eq. (37) becomes

$$dx/d\varphi = y/Q[1 + (dy/dx)^2]. \tag{38}$$

Now, we use the classical formula of Boussinesq for the wave profile

$$y_B(x) = 1 + H_0 \operatorname{sech}^2[(3H_0)^{1/2}x/2]. \tag{39}$$

Substituting Eq. (39) into (38) gives the desired formula for our purpose:

$$dx/d\varphi = (1/Q)(y_B(x)/(1 + [y_B'(x)]^2)) = f(x). \tag{40}$$

Finally, by integrating Eq. (40) numerically, we obtain $x(\varphi)$ along the free surface $A'D'$. The corresponding $y(\varphi)$ along $A'D'$ are then computed from Eq. (39). The interior distribution of y is obtained by solving the Laplace equation (16) using the successive over-relaxation method [11].

Three different mesh sizes were tested, namely 40×10, 60×10 and 50×20. Little difference was observed in the results of the two finer meshes, the difference in y values being less than 0.3 %. Because the surface pressure and corrections dealt with here are small, it is necessary to carry out the computations in double precision. To solve a single problem by this method takes about 1.0 min on the IBM 360/67, including program compilation and execution.

Statistics of a typical calculation ($H_0/d = 0.717$) are shown in Table I, where the

TABLE I

Correction sequence	Maximum absolute value of H_p	Maximum absolute value of R	Wave amplitude H_0/d
0	6.76×10^{-2}	2.33×10^{-2}	.7300000
1	6.31×10^{-2}	3.25×10^{-2}	.7741568
2	1.12×10^{-2}	3.36×10^{-3}	.7307247
3	1.60×10^{-3}	9.92×10^{-4}	.7170046
4	2.89×10^{-5}	1.84×10^{-5}	.7174794
5	9.87×10^{-9}	6.30×10^{-9}	.7174882
6	10^{-14}	10^{-15}	.7174882

Statistics of the computations for the case in which the prescribed discharge $Q = 1.285$. The size of the mesh used was 60×10.

maximum absolute values of $(H_p)_0$ and R_0 are seen to have been reduced from the order 10^{-2} to about 10^{-14}, while the wave amplitude stabilized to the final value $H_0/d = 0.7174882$. Convergence was observed at every grid point of the y field. We found that the rate of convergence accelerates as the residuals become smaller. This type of convergence, called quadratic convergence, is ultimately very fast, in the sense that the number of good decimal digits eventually roughly doubles after each correction until the round-off limit in the computer is reached [8].

It is interesting to note that the formulation as sketched in Fig. 3 has a trivial solution, namely the uniform flow. Thus, it appears that success of the correction method would require a very accurate initial guess of $y(\varphi, \psi)$. However, in Table II we show that a considerable deviation in the initial guess from the true solution

TABLE II

Correction sequence	H_0/d (Case 1)	H_0/d (Case 2)	H_0/d (Case 3)
0	.3700000	.4000000	.4500000
1	.3953959	.3963490	.3991797
2	.3944176	.3944206	.3944828
3	.3944090	.3944090	.3944090
4	.3944090	.3944090	.3944090

For the given parameter $Q = 1.176$ and a mesh with 40×10 grids, three different guesses of the wave amplitude converged to the same solution after three corrections.

can be tolerated. For $Q = 1.1760$ we guessed three different starting values for H_0/d, namely 0.37, 0.40 and 0.45. Computations based on these different guesses converged to the same value $H_0/d = 0.3944090$ after three corrections. Also, the convergence was observed at every grid point of the y field.

Because we can obtain a value of H_0/d corresponding to a specified Q, we are able to compute and plot the wave celerity $C/(gd)^{1/2}$ versus H_0/d for a range of H_0/d. The resulting curve is shown in Fig. 6 and compared with other theories. The experimental data used here are due to Daily and Stephan [1]. The prediction given by the present method appears to be in better agreement with the experiments than other theories. The curve that we have obtained is also very close to the curve given by Laitone [2] which is not shown on our plot.

Daily and Stephan found that Boussinesq's formula (Eq. (39)) gives the most accurate analytic prediction of the wave profile. When $H_0/d > 0.4$, however, the

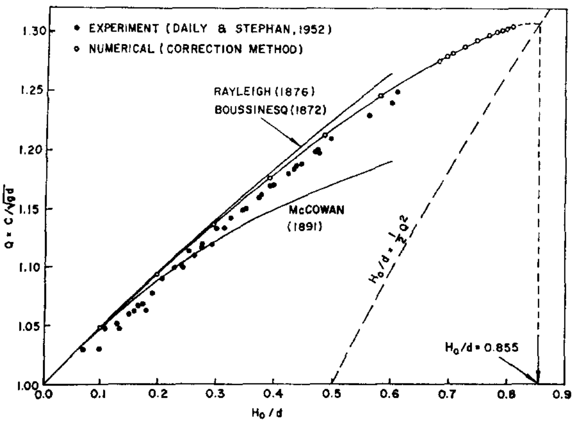

FIG. 6. Comparison of the wave speed.

discrepancy between experiments and Eq. (39) grows. In Fig. 2, the present computed wave profile for $H_0/d = 0.594$ is compared with Boussinesq's profile and measurements. The present solution is in strikingly good agreement with the experiment.

In Figs. 7 and 8, contours of u/C and v/C are plotted for $H_0/d = 0.509$ so that direct comparison with McCowan's theory and Daily and Stephan's data

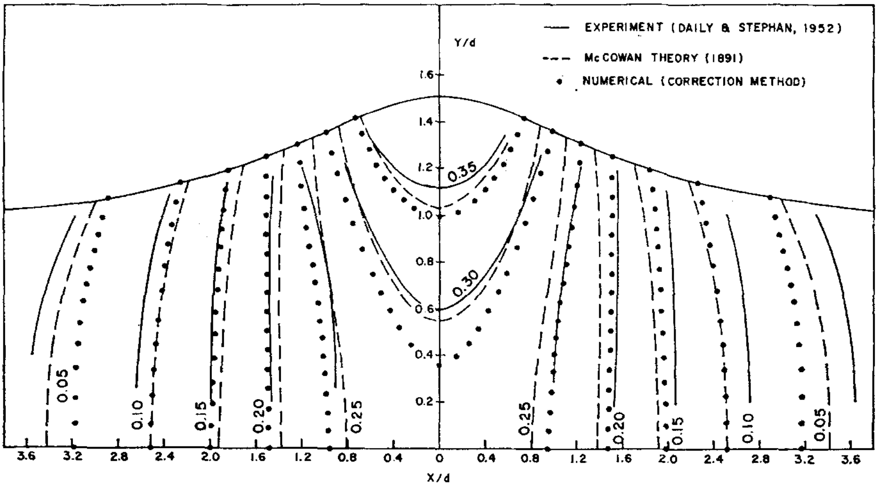

FIG. 7. Comparison of u/C distribution (wave speed $C = 1.217\,(gd)^{1/2}$).

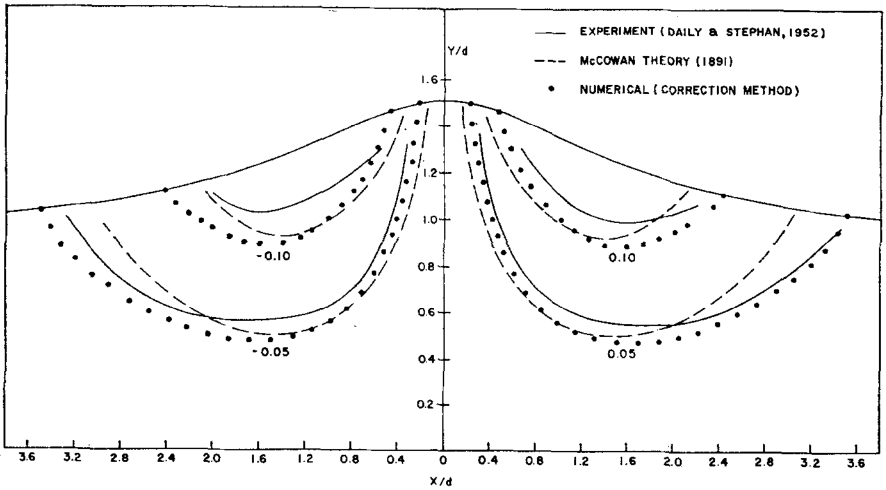

FIG. 8. Comparison of v/C distribution (wave speed $C = 1.217\,(gd)^{1/2}$).

can be made. Considering the difficulty of measuring fluid particle velocities under transient conditions this comparison is only qualitative. Under the wave crest, experimental measurement of u/C is more easily performed than in any other part of the fluid. Comparisons with Daily and Stephan's limited data are shown in Fig. 9 where the theoretical results of McCowan and Laitone are also compared. The conclusion is that the numerical results are very close to experimental data and McCowan's theory in u/C while Laitone's theory tends to overestimate u/C under the wave crest.

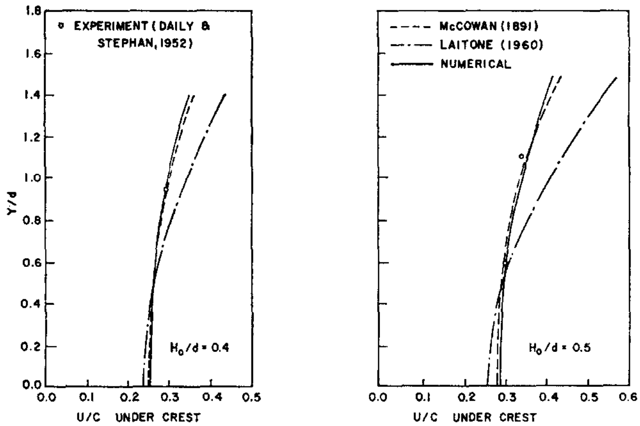

FIG. 9. Comparisons of u/C under the wave crest.

As a part of this investigation, we are also interested in determining the maximum possible value of H_0/d of a solitary wave. The method of guessing $y(\varphi, \psi)$ as outlined above is good for $H_0/d < 0.72$. As a rule, the number of corrections needed to solve the problem increases with an increase in the value of H_0/d. This is simply because the Boussinesq profile Eq. (39) deviates more from the true solution and u along the free surface is quite different from Q/y if H_0/d is large. Therefore, to obtain a wave with $H_0/d > 0.72$ we have to increase the amplitude by increasing the discharge Q gradually. The highest wave thus obtained, the flow pattern of which is shown in Fig. 5, had $H_0/d = 0.81$. For this wave, the velocity head at the crest was $H_V = 0.04$. Thus, this case does not represent the maximum-height wave for which H_V would have to be zero.

Theoretically, $H_V = 0$ cannot be achieved by the method presented here because we have assumed $q^2 \neq 0$ in our previous derivations of the inverse functions $x(\varphi, \psi)$ and $y(\varphi, \psi)$. However, by plotting H_V at the crest versus H_0/d (Fig. 10) and H_V at the crest versus Q (Fig. 11) we can estimate the value of $(H_0/d)_{\max}$ by extrapolation. From Eq. (6) it can be shown that $H_0/d = Q^2/2$ at maximum wave height. Thus, the intersection of the Q versus H_0/d curve and

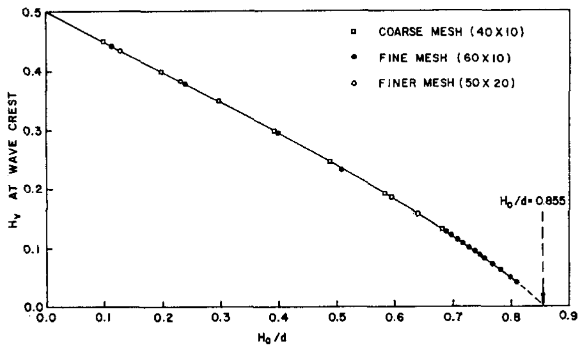

FIG. 10. Extrapolation to find the maximum H_0/d.

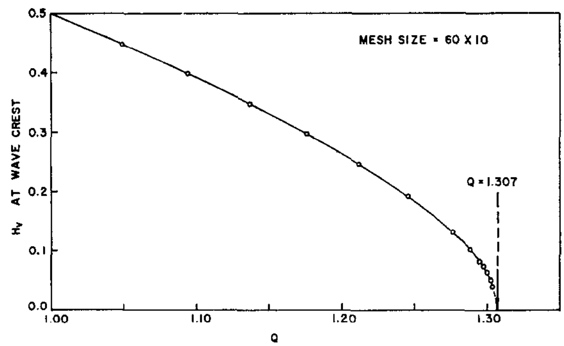

FIG. 11. Extrapolation to find the maximum Q.

$H_0/d = Q^2/2$ curve in Fig. 6 should also yield the maximum value of H_0/d. From these extrapolations, we find $(H_0/d)_{\max} = 0.855$ with the corresponding $Q = 1.307$. Strelkoff [5] and Fenton [4] both obtained $(H_0/d)_{\max} = 0.85$ with $Q = 1.304$.

Finally, the question of selecting a sufficiently large value for φ_∞ (Fig. 3) such that the accuracy of solution is not affected can be settled by a simple experiment. In Fig. 12 we compare the calculated wave profiles corresponding to five different choices of φ_∞. Clearly, the wave profiles converge to a definite shape as φ_∞ is increased.

The method developed here can be applied to many other two-dimensional flow problems. The flow over a smooth step in an open channel of constant width is an example which can be readily analyzed by the present computer program for the solitary wave with only a little modification. A second example is a two-dimensional jet flow under the influence of gravity. It is clear, from our treatment of the solitary wave, that very similar techniques can be employed to study periodic waves of finite amplitude.

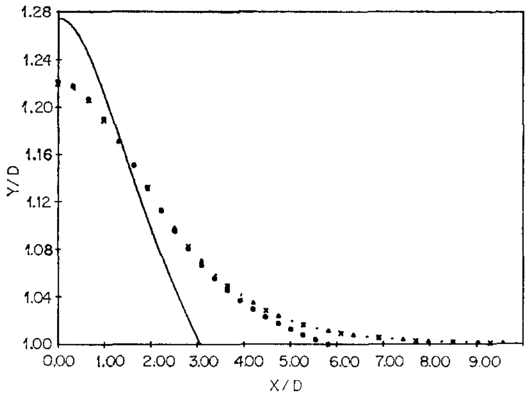

FIG. 12. Convergence of the surface profile as φ_∞ increases. The solid line corresponds to the smallest value for φ_∞. Then the value of φ_∞ is increased according to the following sequence of symbols: ⊙ × ▲ ●.

ACKNOWLEDGMENTS

Special gratitude is due Professor Theodor S. Strelkoff, University of California at Davis, for his original suggestion of the method used in this work. Also, I am greatly indebted to Professor Robert L. Street, Department of Civil Engineering, Stanford University, for his encouragement throughout the course of the present study. This work was carried out by the author at Stanford University as a part of his Engineer thesis.

REFERENCES

1. J. W. DAILY AND S. C. STEPHAN, JR., "The Solitary Wave — Its Celerity, Profile, Internal Velocities and Amplitude Attenuation," Hydro. Lab. Tech. Rept. No. 8, Massachusetts Institute of Technology, June 1952.
2. E. V. LAITONE, The second approximation to Cnoidal and solitary waves, *J. Fluid Mech.* **9** (1960), 430–444.
3. R. GRIMSHAW, The solitary wave in water of variable depth, *J. Fluid Mech.* **46** (1971), 611–622.
4. J. FENTON, A ninth-order solution for the solitary wave, *J. Fluid Mech.* **53** (1972), 257–271.
5. T. S. STRELKOFF, "An Exact Numerical Solution of the Solitary Wave," Proceedings of the 2nd International Conference on Numerical Methods in Fluid Dynamics, Springer–Verlag, 1971.
6. J. G. B. BYATT-SMITH, An exact integral equation for steady surface waves, *Proc. Roy. Soc. (London), Ser. A* **315**, 1970.
7. W. KAPLAN, "Advanced Calculus," Addison–Wesley, 1952.
8. G. FORSYTHE AND C. B. MOLER, "Computer Solution of Linear Algebraic Systems," Prentice Hall, Englewood Cliffs, N. J., 1967.
9. A. RALSTON, "A First Course in Numerical Analysis," McGraw-Hill, New York, 1965.
10. J. J. STOKER, "Water Waves," Interscience Publishers, New York, 1957.
11. G. FORSYTHE AND W. R. WASOW, "Finite Difference Methods for Partial Differential Equations," Wiley, New York, 1960.